Induction of transcription factor Egr-1 gene expression in astrocytoma cells by Murine coronavirus infection

Yingyun Cai, Yin Liu, Xuming Zhang *

Department of Microbiology and Immunology, University of Arkansas for Medical Sciences, 4301 W. Markham Street, Slot 511, Little Rock, AR 72205, USA

Abstract

Mouse hepatitis virus (MHV) causes encephalitis and demyelination in the central nervous system (CNS) of susceptible rodents. Astrocytes are one of the major targets for MHV infection in the CNS, and respond to MHV infection by expressing diverse molecules that may contribute to CNS pathogenesis. Here we characterized the activation of an immediate-early transcription factor Egr-1 by MHV infection in an astrocytoma cell line. We found that the expression of Egr-1 was dramatically increased following virus infection. Using various inhibitors of mitogen-activated protein kinases, we identified that the extracellular signal-regulated kinases 1/2 were involved in the activation of Egr-1 transcription by MHV infection. Experiments with ultraviolet light-inactivated virus revealed that the induction of Egr-1 did not require virus replication and was likely mediated during cell entry. We further found that over-expression of Egr-1 suppressed the expression of BNip3, a pro-apoptotic member of the Bcl-2 family. This finding may provide an explanation for our previously observed down-regulation of BNip3 by MHV infection in astrocytoma cells (Cai, Liu, Yu, and Zhang, Virology 316:104–115, 2003). Furthermore, knockdown of Egr-1 by an siRNA inhibited MHV propagation, suggesting the biological relevance of Egr-1 induction to virus replication. In addition, the persistence/demyelinating-positive strains (JHM and A59) induced Egr-1 expression, whereas the persistence/demyelinating-negative strain (MHV-2) did not. These results indicate a correlation between the ability of MHVs to induce Egr-1 expression and their ability to cause demyelination in the CNS, which may suggest a potential role for the induction of Egr-1 in viral pathogenesis.
© 2006 Elsevier Inc. All rights reserved.

Keywords: Transcription factor Egr-1; Mouse hepatitis virus; Murine coronavirus; Astrocytoma cells; Gene expression; Signal transduction

Introduction

Murine coronavirus mouse hepatitis virus (MHV) is a member of the family *Coronaviridae*, which is a group of enveloped, single-stranded, and positive-sense RNA viruses. MHV utilizes its surface spike (S) glycoprotein to initiate infection by interacting with a specific cellular receptor (Williams et al., 1991). This interaction triggers a conformational change of the spike, resulting in exposure of its fusogenic domain, which further triggers fusion between viral envelope and plasma membrane and subsequent release of the nucleocapsid into cytoplasm (Matsuyama and Taguchi, 2002). In some MHV strains, virus entry occurs following receptor-mediated endocytosis (Nash and Buchmeier, 1997). The precise process of virus uncoating is not clear, but is believed to involve

dephosphorylation of the nucleocapsid (N) protein and dissociation of N protein from viral genomic RNA (Kalicharran et al., 1996). The incoming viral genomic RNA is then translated into the viral polymerase polyprotein of more than 800 kDa that is essential for subsequent viral replication and transcription.

MHV can infect rodents and cause hepatitis, nephritis, enteritis, and central nervous system (CNS) diseases (Sebesteny and Hill, 1974; Herndon et al., 1975). In the CNS, MHV infection causes encephalitis and demyelination. Because the pathology of demyelination caused by MHV infection resembles those of multiple sclerosis (MS) seen in humans, MHV has been extensively used as an animal model for MS and other neurodegenerative diseases (Lampert et al., 1973; Herndon et al., 1977). Following MHV infection, mice usually develop acute encephalitis and demyelination during the first week of infection (Woyciechowska et al., 1984). Most of the viruses are cleared from the CNS at the end of the second week post-

---

* Corresponding author. Fax: +1 501 686 5359.
E-mail address: zhangxuming@uams.edu (X. Zhang).

infection (p.i.). If the mice survive the acute phase, chronic demyelination then develops and reaches to a peak at around 30 days p.i. At this time, however, infectious virus can no longer be isolated but viral RNAs are still detectable in the CNS (Fleming et al., 1993; Adami et al., 1995). Viral RNA can persist in the CNS, especially in astrocytes, for an extended period of time (Adami et al., 1995; Perlman and Ries, 1987; Rowe et al., 1998).

Astrocytes play important roles in supporting the nervous system and controlling the chemical and ionic environment of the CNS. Astrocytes can be stimulated to produce diverse pro-inflammatory molecules such as cytokines, chemokines, and nitric oxide (Van Wagoner and Benveniste, 1999; Huang et al., 2000; Chen and Swanson, 2003). It has been shown that MHV infection can induce the expression of transforming necrosis factor (TNF)-α, interleukin (IL)-6, matrix metalloproteinases, and inducible nitric oxide synthase (iNOS) in astrocytes (Kyuwa et al., 1994; Joseph et al., 1993; Zhou et al., 2001; Grzybicki et al., 1997). Infection of astrocytes with MHV may thus modulate the development of the CNS pathology and alter the course of the disease. In vitro, MHV can persist in the DBT astrocytoma cell line, in the progenitor oligodendrocyte/astrocyte CG-4 cells and in a fibroblast 17Cl-1 cell line (Chen and Baric, 1995; Liu and Zhang, 2005; Maeda et al., 1995; Sawicki et al., 1995). However, the precise mechanisms of viral persistence in animal CNS and in cultured cell lines are not known. Previous studies have suggested that alteration of receptor expression in DBT and 17Cl-1 cells by MHV infection may facilitate viral persistence (Chen and Baric, 1996; Porntadavity et al., 2001; Sawicki et al., 1995). In our previous analysis on cellular gene expression in MHV-infected DBT cells using the DNA microarray technology, we suggested that alterations of the expression of cellular genes, in addition to the receptor down-regulation, might play an important role in establishing persistent infection in DBT cells (Cai et al., 2003).

One of such candidate cellular factors is the early growth regulator-1 (Egr-1). Egr-1 is also named as nerve growth factor induced-A (NGFI-A), zif268, TIS8, or Krox24, which is an immediate early gene, the prototype of a family of zinc-finger transcription factors (Waters et al., 1990; Changelian et al., 1989; Christy and Nathans, 1989; Varnum et al., 1989; Lemaire et al., 1990). Egr-1 can be rapidly induced by diverse stimuli, including growth factors, hormones, cytokines, neurotransmitters and injurious stimuli through different mitogen-activated protein kinases (MAPKs) pathways, including the extracellular signal-regulated kinase (ERK), c-Jun NH_2-terminal kinase (JNK), and p38 MAPK pathways depending on the stimuli (Sukhatme et al., 1988; Cao et al., 1990, 1992; Lim et al., 1998; Milbrandt, 1987; Honkaniemi et al., 1995). For example, Egr-1 gene expression is induced through ERK signal pathway by cytokines and growth factors, while it is induced via p38 and JNK pathways by stress treatment such as heat shock, sodium arsensite, ultraviolet, radiation, and anisomycin (Santiago et al., 1999; Liu and Zhang, 2005). As a transcription factor, Egr-1 contains a DNA binding domain, which binds specifically to the consensus binding sequence GCG (T/G) GGGCG (Cao et al., 1990). Egr-1 can induce the expression of a number of genes,

such as platelet-derived growth factor (PDGF)-A and -B, macrophage colony-stimulating factor (M-CSF), TNF-α, IL-2, and intercellular adhesion molecule (ICAM)-1 (Delbridge and Khachigian, 1997; Khachigian et al., 1996; Harrington et al., 1991; Kramer et al., 1994; Skerka et al., 1995; Maltzman et al., 1996). All of these genes contain one or more Egr-1 consensus binding sites within their promoter regions. Thus, Egr-1 is involved in regulation of a variety of cellular processes, including cell proliferation, differentiation, neuronal plasticity, vascular wound response, and cancer progression (Hill and Treisman, 1995; Nguyen et al., 1993; James et al., 2004; Khachigian et al., 1996; Kobayashi et al., 2002). For examples, it has been demonstrated that astrocyte growth is regulated by neuro-peptides through basic fibroblast growth factor and Egr-1 (Hu and Levin, 1994; Biesiada et al., 1996); Egr-1 was significantly increased in prostate carcinoma and treatment with anti-Egr-1 anti-sense dramatically inhibited the prostate cancer progression, suggesting a role for Egr-1 in the development of prostate cancer (Eid et al., 1998; Baron et al., 2003a,b).

In the present study, we investigated the expression of Egr-1 in MHV-infected DBT cells, the signal pathways that induce Egr-1 expression, and the potential outcome of Egr-1 expression on cell survival and viral persistence. We found that both mRNA and protein levels of Egr-1 were significantly induced in DBT cells by MHV infection, which was mediated through the ERK signal pathway. Moreover, the ability of MHV strains to induce Egr-1 expression was correlated with their ability to cause persistent infection in the CNS. Our data may thus suggest a link between the induction of Egr-1 gene expression and the establishment of viral persistence in DBT cells. These findings may also provide insight into the mechanisms by which MHV establishes persistence in the DBT cells and in animal CNS.

Results

Induction of the transcription factor Egr-1 expression in astrocytoma DBT cells by MHV infection

In a previous study, we performed DNA microarray analysis to determine the alteration of cellular gene expression by MHV infection in DBT cells (Cai et al., 2003). We found that the expression of a substantial number of genes was altered by MHV infection. Among them, the expression of the transcription factor Egr-1 was increased more than 9-fold (data not shown). To verify the microarray data, we used RT-PCR to directly determine the Egr-1 mRNA during the course of virus infection. DBT cells were infected with MHV-JHM strain at an m.o.i. of 5 or mock-infected. The intracellular RNAs were isolated at various time points p.i. cDNAs were synthesized by RT with a random primer and were amplified by PCR using a primer pair specific to Egr-1 or β-actin as an internal control. As shown in Fig. 1A, the cDNAs representing Egr-1 gene were not induced at 4 h p.i., but were dramatically increased (a 46-fold increase) at 8 h p.i., and peaked at 12 h p.i. At 16 h p.i., the level of Egr-1 mRNA appeared to decline. In contrast, the level of β-actin mRNA
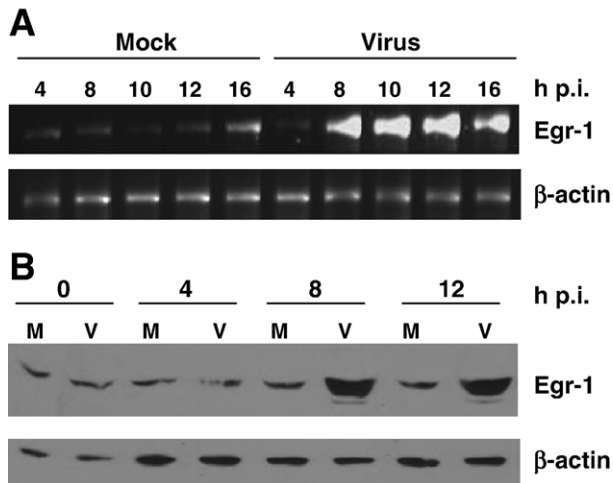
Fig. 1. Induction of transcription factor Egr-1 expression by MHV-JHM infection. DBT cells were infected with MHV-JHM strain at an m.o.i. of 5 or mock-infected. For mRNA detection (A), intracellular RNAs were isolated at various time points p.i. as indicated. RT-PCR was performed to detect the mRNAs of Egr-1 gene and β-actin, the latter of which was served as an internal control. The RT-PCR products were analyzed by electrophoresis on 2% agarose gel and visualized by staining with ethidium bromide. Images were taken with the digital camera (UVP). For protein detection (B), cells were lysed at various time points p.i. as indicated. Equal amounts of cell lysates were separated by polyacrylamide gel (9%) electrophoresis. Proteins were then transferred to nitrocellulose membranes and were detected with an Egr-1 antibody and enhanced chemiluminescence by Western blot analysis. An aliquot of an equal amount of cell lysates from each sample was used for analyzing the β-actin protein with the β-actin antibody as an internal control. The data are representative of three independent experiments. M, lysates from mock-infected cells; V, lysates from MHV-JHM-infected cells.

remained relatively constant from 4 to 16 h p.i. These results demonstrate that the expression of Egr-1 gene was induced by MHV infection at the transcriptional level, which confirmed the finding obtained from microarray analysis.

Next, Western blot was employed to detect Egr-1 protein. Following infection, DBT cells were harvested and lysed at various time points p.i. Immunoblotting with the anti-Egr-1 antibody or anti-β-actin antibody was performed. As expected, a significant increase ($\approx$20-fold) in Egr-1 protein was detected in virus-infected cells at 8 and 12 h p.i. but not at 4 h p.i., as compared to those in mock-infected cells (Fig. 1B). Taken together, these data demonstrate that Egr-1 gene expression was significantly induced in DBT cells by MHV infection.

Both live and UV-inactivated MHVs were capable of inducing Egr-1 gene expression

To determine whether the induction of Egr-1 expression requires viral replication, UV-irradiated virus was used in comparison with live virus infection. UV-irradiated virus can bind to cell receptors and penetrate into the cells, but is unable to replicate. DBT cells were infected with UV-irradiated virus or live virus, or mock-infected. Total intracellular RNAs were isolated at 8 and 12 h p.i. RT-PCR was performed to determine the expression of Egr-1 mRNA. As shown in Fig. 2, Egr-1 mRNA was induced by infection with the live virus at 8 and

12 h p.i. Although infection with UV-inactivated virus did not significantly induce Egr-1 expression at 8 h p.i., it did so by 12 h p.i. ($\approx$20-fold increase as compared to mock-infected cells), indicating that virus replication is not absolutely required for Egr-1 induction. The data also suggest that virus entry alone is sufficient to induce Egr-1 expression, albeit with a low efficiency.

The induction of Egr-1 was mediated by virus infection through the ERK signal pathway

It has been previously reported that both p38 and JNK MAPKs were activated in DBT cells infected with MHV-JHM during viral replication (Banerjee et al., 2002). It has also been shown that ERK was activated in peritoneal exudative macrophages at a very early time point of infection (5 min p.i.) with MHV-3 (McGilvray et al., 1998). As described in the introduction, Egr-1 can be induced by all three MAPK pathways. It was therefore interesting to determine whether MHV-induced Egr-1 gene expression was mediated through one or more of the three MAPK signaling pathways. To address this question, we determined the activation of Egr-1 by MHV infection following the treatment of cells with inhibitors specifically inhibiting one of the three MAPK pathways. UO126 is the inhibitor of the ERK pathway, whereas SB203580 and SP600125 are the inhibitors of p38 and JNK pathways, respectively (Cuenda et al., 1995; Bennett et al., 2001; Favata et al., 1998). DBT cells were treated with UO126 (25 μM or 50 μM), SB203580 (40 μM), SP600125 (40 μM), or DMSO (as a negative control) for 1 h prior to infection, during and throughout the infection. Cells were infected with MHV-JHM at an m.o.i. of 5 or mock-infected. Intracellular RNAs were harvested at 12 h p.i., and Egr-1 mRNAs were detected by RT-PCR. As shown in Fig. 3A, treatment of cells with UO126 at either concentration (25 μM or 50 μM) almost completely blocked the induction of Egr-1 by MHV infection. By contrast, treatment with SB203580 or SP600125 failed to block Egr-1 induction by MHV infection. To verify this finding, we used a
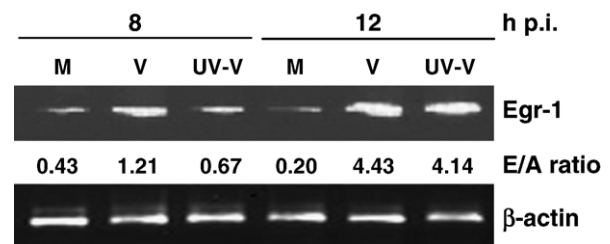

Fig. 2. Egr-1 mRNA expression was induced by both live and UV-irradiated viruses. DBT cells were infected with live or UV-irradiated MHV-JHM or mock-infected. Intracellular RNAs were isolated at 8 and 12 h p.i. RT-PCR was performed to detect Egr-1 mRNA. β-actin was used as an internal control. The RT-PCR products were analyzed by electrophoresis on 2% agarose gel and visualized by staining with ethidium bromide. Images were taken with the digital camera (UVP). The intensity of each band was quantified and the ratio of Egr-1 to β-actin for each sample was presented as E/A ratio. The data are representative of three independent experiments. M, RNAs from mock-infected cells; V, RNAs from MHV-JHM-infected cells; UV-V, RNAs from UV-irradiated MHV-JHM-infected cells.
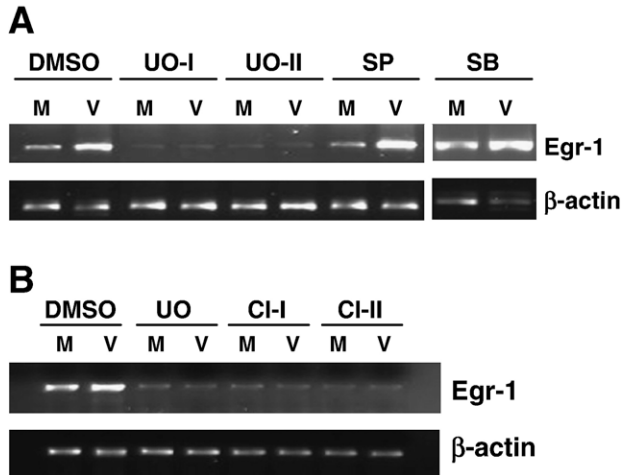
A

B

Fig. 3. The induction of Egr-1 gene by MHV infection was mediated through the ERK signal pathway. (A) DBT cells were pre-treated with MEK inhibitor UO126 (I: 25 μM or II: 50 μM), JNK inhibitor SP600125 (40 μM), p38 inhibitor SB203580 (40 μM), or DMSO for 1 h prior to infection. These treated cells were then infected with MHV-JHM at an m.o.i. of 5 or mock-infected. At 12 h p.i., the intracellular RNAs were isolated and were subjected to RT with a random primer. cDNAs were amplified by PCR using the primer pair specific to Egr-1 or β-actin (as an internal control). The drugs were present in the medium throughout the 12 h period. The data are representative of three independent experiments. M, RNAs from mock-infected cells; V, RNAs from MHV-JHM infected cells. (B) As in panel A, except that the ERK1/2 inhibitor CI-1040 (CI-I: 3 μM; CI-II: 5 μM) was used and that the concentration of UO126 was 50 μM in this experiment.

new inhibitor, CI-1040, which has been shown to be even more specific and potent to the ERK pathway (Sebolt-Leopold et al., 1999). We found that treatment of DBT cells with CI-1040 (3–5 μM) blocked the induction of Egr-1 by MHV infection to a level similar to those treated with UO126 at 50 μM (Fig. 3B). We thus conclude that induction of Egr-1 gene expression by MHV infection was likely mediated through the MEK-ERK signal pathway.

Activation of the ERK signal pathway by MHV infection

Although the above studies with MAPK inhibitors pointed out the involvement of ERK pathway in Egr-1 induction, it is not known whether the ERK pathway is actually activated by MHV infection. To provide direct evidence for the activation of the ERK pathway, we determined the phosphorylation status of ERK1 (p44) and ERK2 (p42) following MHV infection. Because it is well known that serum can stimulate ERK activation, DBT cells were subjected to serum-starvation for 24 h prior to virus infection. DBT cells were then infected with gradient-purified MHV-JHM at an m.o.i. of 5 or mock-infected. After 1 h binding at 4 °C, the viral inoculums were removed. Cells were fed with fresh medium without serum and were incubated at 37 °C. At various time points as indicated, cell lysates were prepared for determination of ERK1/2 phosphorylation by Western blot analysis. As shown in Fig. 4, although ERK1/2 phosphorylation was detected in both virus-infected and mock-infected cells at all time points p.i., the levels of phosphorylation were significantly higher in virus-infected cells

than in mock-infected cells from 5 to 120 min p.i. Moreover, no increase in ERK1/2 phosphorylation was detected in virus-infected cells at 0 min p.i. Taken together, these data indicate that the ERK signal pathway was indeed specifically activated by MHV-JHM infection.

Over-expression of Egr-1 repressed BNip3 promoter activity

We have demonstrated in a previous study that the expression level of the pro-apoptotic gene BNip3 was down-regulated by MHV infection (Cai et al., 2003). A recent report showed that BNip3 gene expression was down-regulated by over-expression of Egr-1 in prostate cancer cells (Virolle et al., 2003). Therefore, it is of interest to determine whether the down-regulation of BNip3 in MHV-infected DBT cells is also mediated through the induction of the transcription factor Egr-1. First, we determined the BNip3 promoter activity by using the luciferase reporter assay (Cai et al., 2003). We expressed Egr-1 protein transiently in DBT cells by cotransfecting pBS-CMV-Egr-1, which contains the Egr-1 ORF under the control of a CMV promoter, and pGL3-BNip3 reporter plasmid (Bruick, 2000; Cai et al., 2003). After 20 h post-transfection, cell lysates were harvested and luciferase activity determined. Results showed that transient cotransfection with an increased amount of Egr-1-expressing plasmid (ranging from 20 to 500 ng per well) exhibited an increased inhibitory effect on BNip3 promoter activity by 2 to 45% (Fig. 5A). This inhibition appeared to be specific for Egr-1 because cotransfection with the empty vector pBS-CMV (without expressing the Egr-1) did not have any effect on luciferase activity (Fig. 5A). The specific inhibitory effect of the expressed Egr-1 on pGL3-BNip3 reporter was further examined in a cotransfection experiment, in which pBS-CMV-Egr-1 or pBS-CMV and the pSV-β-gal reporter plasmid (which is under the control of an SV40 promoter) were cotransfected into DBT cells. At 24 h post-transfection, β-gal activity was determined. In stark contrast to the result for pGL3-BNip3 reporter (Fig. 5A), the β-gal activity was virtually unaffected by the expression of Egr-1 (Fig. 5B).
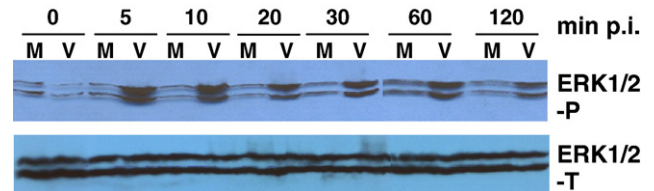

Fig. 4. Activation of ERK signaling pathway by MHV infection. DBT cells were infected with purified MHV-JHM at an m.o.i. of 5 or mock-infected. After 1 h binding at 4 °C, the viral inoculums were removed and fresh medium without serum were added to the plates. The cells were harvested and lysed following incubation at 37 °C for various time points p.i. as indicated. Equal amounts of cell lysates were separated by polyacrylamide gel (10%) electrophoresis. Proteins were then transferred to nitrocellulose membranes and were detected with an antibody specific for phosphorylated-forms of ERK1/2 (ERK1/2-P) and enhanced chemiluminescence by Western blot analysis. An aliquot of an equal amount of cell lysates from each sample was used for analyzing total ERK1/2 (ERK1/2-T) with an antibody specific for ERK1/2 as an internal control. The data are representative of three independent experiments. M, lysates from mock-infected cells; V, lysates from MHV-JHM-infected cells.
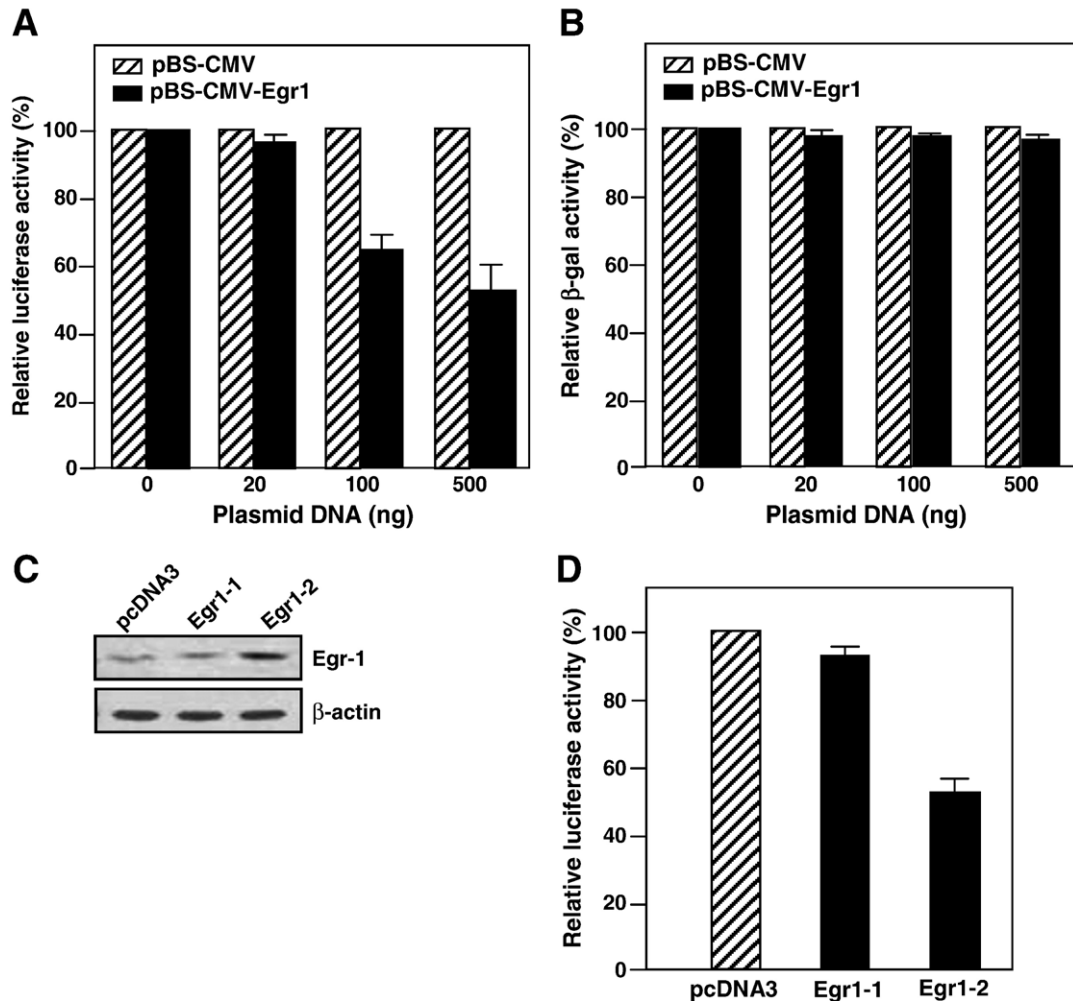
Fig. 5. Inhibition of the BNip3 promoter activity by over-expression of Egr-1. (A) BNip3 promoter activity in transiently transfected cells. DBT cells were transiently cotransfected with the Egr-1 expression plasmid (pBS-CMV-Egr-1) or empty vector (pBS-CMV) at an amount of 0, 20, 100, or 500 ng per well and pGL3-BNip3 reporter plasmid at 500 ng per well. After 20 h post-transfection, cell lysates were harvested, and the luciferase activity was measured. The relative luciferase activity in pBS-CMV-Egr-1-expressing cells is indicated as percentage of the luciferase activity expressed from pBS-CMV-transfected cells, which was set as 100%. Data are the average of a triplicate experiment and are representative of 3 independent experiments. (B) Effect of Egr-1 on SV40 promoter activity. The experiments were performed exactly as in panel A except that the cotransfecting reporter plasmid is pSV-β-gal instead of pGL3-BNip3. (C) Stable expression of Egr-1 in DBT cells. DBT cells were transfected with the Egr-1 expression plasmid (pcDNA3-Egr1) or with empty vector (pcDNA3). Following selection with G418 for more than 1 month, two clones stably expressing Egr-1 were obtained. The expression levels of these two clones were determined by Western blot with an antibody specific to Egr-1. β-actin protein serves as an internal control. (D) BNip3 promoter activity in Egr-1-stable expressing cells. Equal numbers of cells from these two cloned cells or cells stably transfected with pcDNA3 empty vector were cotransfected with pGL3-BNip3 reporter plasmid and pSV-β-gal plasmid, the latter of which was used as a control for transfection efficiency. After 24 h post-transfection, the luciferase activity and β-gal activity were measured. The relative luciferase activity in Egr-1-expressing cells (Egr1-1 and Egr1-2) is indicated as percentage of the luciferase activity expressed from pcDNA3-transfected cells, which was set as 100%. The luciferase activity was normalized with β-gal activity. Data are the average of three independent experiments and error bars denote standard deviation.

Thus, over-expression of Egr-1 selectively inhibited BNip3 promoter activity.

To further confirm these results, we established cell lines that stably express Egr-1 protein. We tested two cell clones, which expressed different amounts of Egr-1 protein. Clone #2, termed Egr-1–2, expressed higher level of Egr-1 protein than clone #1, termed Egr-1–1, which expressed almost the same amount of Egr-1 protein as the cells stably transfected with the empty vector pcDNA3 plasmid (Fig. 5C). Equal numbers of these cloned cells were cotransfected with pGL3-BNip3 reporter plasmid and pSV-β-gal plasmid, the latter of which served as a

control for transfection efficiency as well as for specificity. At 24 h post-transfection, luciferase and β-gal activities in the cells were determined, and the luciferase activity was normalized to β-gal activity, which was essentially unaffected by the cotransfection. As shown in Fig. 5D, BNip3 promoter activity was decreased approximately 45% in Egr-1–2 clone, while it decreased only 7% in Egr-1–1 clone as compared to those in vector-control cells (lane pcDNA3). These results demonstrate that over-expression of Egr-1 repressed the expression of the pro-apoptotic BNip3 gene, thus suggesting that the previously observed down-regulation of BNip3 expression in DBT cells by

negative control and for monitoring the transfection efficiency. At various times post-transfection, the protein level of Egr-1 was monitored by Western blot analysis. A representative result obtained at 60 h post-transfection is shown in Fig. 6A. In the absence of virus infection, the Egr-1 level was significantly lower in Egr-1-siRNA-transfected cells than in EGFP-siRNA-transfected cells, demonstrating the effectiveness and specificity of the Egr-1-siRNA. Similarly, Egr-1 expression was effectively blocked by Egr-1-siRNA but not by EGFP-siRNA even in the presence of virus infection. Egr-1 protein was much higher in virus-infected cells than in mock-infected cells when the cells were transfected with the EGFP-siRNA, further confirming that MHV infection induces Egr-1 expression. We then determined the effect of Egr-1 knockdown on virus propagation. Indeed, knockdown of Egr-1 expression by Egr-1-siRNA exhibited a detrimental effect on virus propagation, reducing the virus titer by approximately 2 log10 (Fig. 6B). Interestingly, apoptotic cells were increased in virus-infected, Egr-1 knockdown cells as compared to the control cells that were transfected with the EGFP-siRNA (Fig. 6C). Although the increase was statistically significant ($p = 0.037$), the level of the increase was extremely low, which may result from a number of factors. For example, in
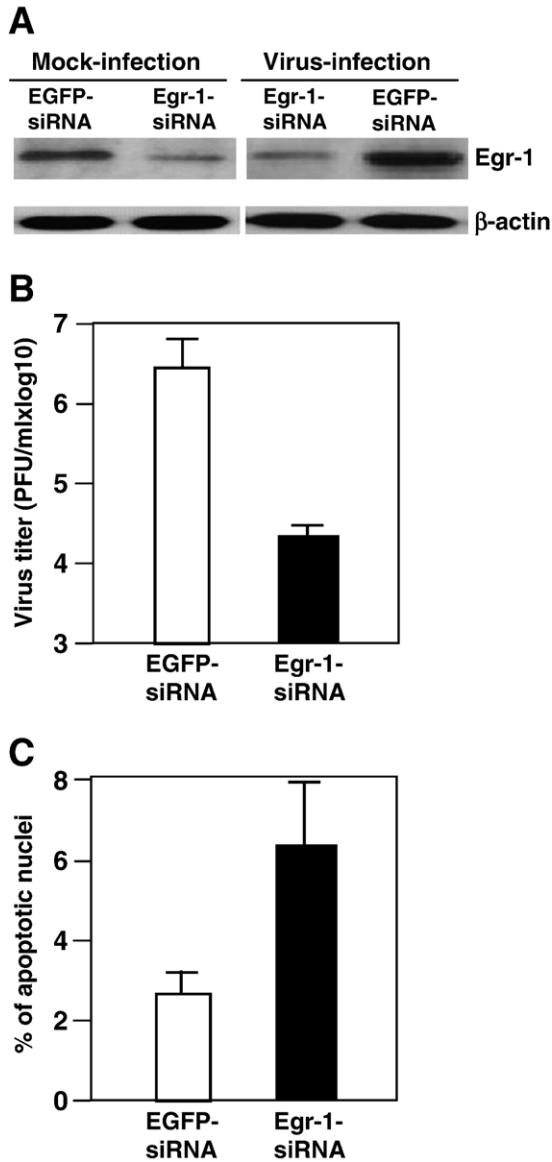
Fig. 6. Effect of Egr-1 knockdown on virus propagation and cell survival. (A) Effect of Egr-1-siRNA on Egr-1 expression. DBT cells were transfected with Egr-1-siRNA or EGFP-siRNA for 60 h, and then infected with MHV or mock-infected with PBS. Cells were lysed at 16 h p.i. and proteins were detected by Western blot with anti-Egr-1 or anti-β-actin antibodies (A). Virus titers were determined by virus plaque assay at 16 h p.i. and were expressed as mean±standard deviation (SD) of three experiments (B). (C) Apoptosis was assessed by determining the apoptotic nuclei following propidium iodide staining, and was expressed as mean percentage of the cell population and SD of three experiments. Statistical analysis indicates significance between the Egr-1 knockdown cells and the control cells ($p = 0.037$).

MHV-infection was likely mediated through up-regulation of Egr-1 expression.

Role of Egr-1 in virus propagation and cell survival

To establish the biological relevance of the Egr-1 induction, we used an siRNA specific to Egr-1 to knockdown Egr-1 in DBT cells. Cells were transfected with an Egr-1-siRNA or a non-specific EGFP-siRNA, the latter of which serves both as a
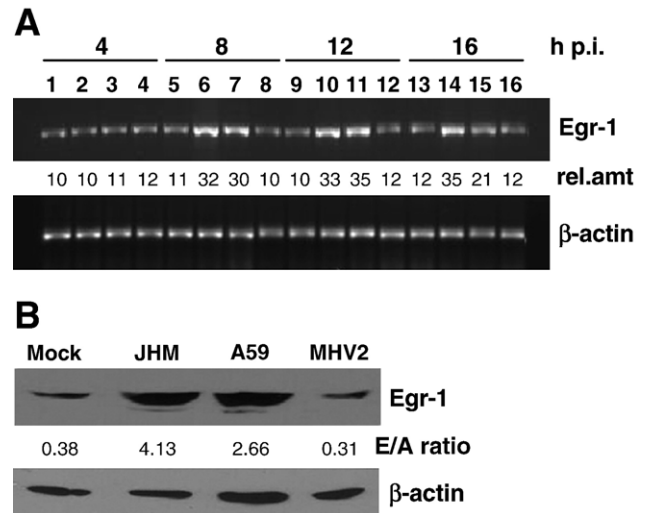

Fig. 7. Differential induction of Egr-1 expression by different MHV strains. (A) Expression of Egr-1 mRNA. DBT cells were infected with different strains of MHVs (including MHV-JHM, A59 and MHV2) or mock-infected. Total intracellular RNAs were isolated at various time points p.i. as indicated. RT-PCR was performed to detect the Egr-1 mRNA. β-actin was used as an internal control. The RT-PCR products were analyzed by electrophoresis on 2% agarose gel and visualized by staining with ethedium bromide. Images were taken with the digital camera (UVP). Lanes 1, 5, 9, and 13: RNAs from mock-infected cells; Lanes 2, 6, 10, and 14: RNAs from cells infected with MHV-JHM; Lanes 3, 7, 11, and 15: RNAs from cells infected with MHV-A59; Lanes 4, 8, 12, and 16: RNAs from cells infected with MHV-2. The intensity of each band was quantified by densitometry (UVP), which is indicated as relative amount (rel. amt) shown beneath each lane. (B) Detection of Egr-1 protein. DBT cells were infected as in panel A. Cells were harvested and lysed at 12 h p.i. Equal amounts of the cell lysates were separated by polyacrylamide gel (9%) electrophoresis. Western blot was performed to detect Egr-1 and β-actin proteins by using an antibody specific to Egr-1 and β-actin, respectively. The intensity of each band was quantified and the relative quantity was expressed as a ratio of Egr-1 to β-actin (E/A ratio) for each sample.

siRNA-expressing cells, not only was Egr-1 much lower (Fig. 6A) but also was the virus replication (Fig. 6B). Thus, very low level of virus replication might not be able to induce robust apoptosis. Nevertheless, these results indicate that Egr-1 may play a role in virus replication and cell survival.

Induction of Egr-1 gene expression by MHV infection was correlated with the abilities of the viruses to cause persistent infection

Both MHV-JHM and MHV-A59 are demyelinating-positive strains and can cause persistent infection in the CNS of infected rodents, whereas MHV-2 is a non-demyelinating strain and does not cause persistent infection. To test the hypothesis in cell culture that cellular gene expression altered by MHV infection may contribute to the control of virus replication and persistence in CNS cells and consequently to viral pathogenicity, we determined whether MHV strains with distinctive pathogenic phenotypes have different abilities to induce Egr-1 expression. DBT cells were infected with different strains of MHV (including MHV-JHM, -A59 and MHV2) or mock-infected. Total intracellular RNAs were isolated at different time points p.i. as indicated, and the RNA level of Egr-1 gene was determined by RT-PCR. As shown in Fig. 7A, Egr-1 mRNA was induced (approximately 3 fold) by both MHV-JHM and MHV-A59 at 8, 12, and 16 h p.i., but not at 4 h p.i. In contrast, infection with MHV-2 failed to induce Egr-1 expression as compared to those of mock-infected cells (compare lanes 4, 8, 12, and 16 with lanes 1, 5, 9, and 13 in Fig. 7A). We also performed Western blot to detect the protein expression. As presented in Fig. 7B, Egr-1 protein was significantly increased in both JHM- and A59-infected cells ($\approx$ 11- and 7-fold increase, respectively) but not in MHV-2-infected cells. These data provide evidence that correlates the ability of the MHV strains to induce Egr-1 expression with their ability to cause persistent infection in the CNS cells and demyelinating disease in the animal CNS.

Discussion

In the present study, we have demonstrated that MHV infection of DBT cells induced the expression of transcription factor Egr-1 as determined by RT-PCR and Western blot. These results confirmed our previous findings obtained from DNA microarray analysis (Cai et al., 2003). As an immediate-early gene, Egr-1 can be rapidly induced by a variety of stimuli, including virus infections. Indeed, in addition to MHV as found in this study, it has been shown that Egr-1 gene expression is induced by infections with diverse groups of viruses. For example, Egr-1 expression was induced in the brain tissue in experimental mice infected with Rabies virus and Borna disease virus (BDV), in a number of human cells infected with human foamy virus (HFV), in human T-cell leukemia virus type 1-(HTLV-1) or type 2 (HTLV-2)-transformed cell lines, in B-lymphocytes infected with Epstein–Barr virus (EBV), and in Bc-2 cells latently infected with Kaposi's sarcoma-associated herpesvirus (KSHV) (Fu et al., 1993; Wagner et al., 2000; Calogero et al., 1996; Wright et al., 1990; Sukhatme et al., 1988).

How is the Egr-1 expression induced by virus infection? In HTLV-transformed cells, it appears that the Tax protein is responsible for the induction of Egr-1 expression (Fujii et al., 1991). As a transactivator, Tax can interact with the transcription factor CREB/ATF and serum response factors (SRFs) (Suzuki et al., 1993; Fujii et al., 1992). These factors in turn interact with the CREB/ATF response element (CRE) and serum response element (SRE), respectively, on the promoter of Egr-1, thus activating the expression of Egr-1 (Fujii et al., 1991; Sakamoto et al., 1992). In the case of MHV-infected cells, we demonstrated the activation of ERK by MHV infection and the inhibition of Egr-1 expression by the MEK1/2 inhibitors (Figs. 4 and 3). Our results thus suggest that the induction of Egr-1 expression upon MHV infection is likely mediated through the ERK signaling pathway. It is well established that the activation of ERK can activate its downstream transcription factor Elk, which then interacts with SRFs and activates a number of immediate-early genes whose promoters contain an SRE. Therefore, we postulate that the induction of Egr-1 by MHV infection might follow the ERK1/2 → Elk → SRFs → Egr-1 pathway. The upstream signal(s) that activates ERK1/2 has not been determined in this study although the inhibitor that we used to block ERK activation acts on the upstream kinase MEK1/2. Nevertheless, our data suggest that the upstream signal(s) most likely resides within or in the vicinity of the cytoplasm membranes, which is activated during virus entry. There are two pieces of evidence supporting this interpretation. First, infection with UV-inactivated virus was still capable of inducing Egr-1 transcription (Fig. 2). Second, ERK1/2 was activated within 5 min upon virus entry and during the first 2 h p.i. (Fig. 4). Although live virus is a stronger inducer for Egr-1 expression than UV-inactivated virus, ERK1/2 activation was no longer detected at 3 h following infection (data not shown). This suggests that although virus replication may play a role in the induction of Egr-1 activation, the predominant signal that activates Egr-1 expression is likely triggered during cell entry. Activation of ERK1/2 has also been observed between 5 and 45 min p.i. in peritoneal exudative macrophage infected with MHV-3 (McGilvray et al., 1998). Although Banerjee et al. (2002) did not detect ERK1/2 activation after 2 h p.i., they did not perform the same experiments at earlier time points.

Despite different mechanisms for Egr-1 induction by diverse groups of viruses as discussed above, the finding that Egr-1 is up-regulated by these different viruses may suggest that infections by these viruses may have some common consequences on both viruses and host cells. One of the potential consequences is to facilitate virus replication in the host cells. Indeed, knockdown of Egr-1 by siRNA significantly impaired MHV propagation (Fig. 6B). It has also been reported that there is a good correlation between Egr-1 and viral RNA expressions in the mouse brains infected with Rabies and Borna disease viruses, which raises the possibility that Egr-1 expression may induce some phenotypic changes in neurons that render them more susceptible to viral replication (Fu et al., 1993). The other potential consequence of Egr-1 induction is to promote host cell

proliferation and survival. It has been suggested that the induction of Egr-1 expression in EBV-infected B lymphocytes, in EBV-transformed lymphoma and in HTLV-transformed cell lines, may facilitate cell growth and may play a role in tumorigenesis (Calogero et al., 1996; Fujii et al., 1991; Sakamoto et al., 1992). It has also been suggested that the expression of Egr-1 may change the phenotype of the infected cells, which may help KHSV to establish latency (Sun et al., 2001). By analogy, the induction of Egr-1 by MHV infection may also facilitate the survival of the infected cells, thereby promoting the establishment of MHV persistence in glial cells. In support of this hypothesis is our finding that over-expression of Egr-1 suppresses the expression of the pro-apoptotic gene BNip3 (Fig. 5) that is down-regulated by MHV infection as demonstrated in our previous study (Cai et al., 2003), whereas knockdown of Egr-1 leads to apoptosis when cells are infected with MHV (Fig. 6C).

The induction of Egr-1 expression by MHV infection may also contribute to viral pathogenicity. Both JHM and A59 are able to cause acute encephalitis and demyelination and persistence in the CNS, whereas MHV-2 cannot. Recent studies from our laboratory and others suggest that the ability of MHV strains to cause acute encephalitis is correlated with their ability to induce proinflammatory cytokines, particularly TNF-α and IL-6, in primary mouse astrocytes and microglia (Li et al., 2004; Yu and Zhang, in press). Interestingly, an Egr-1 binding site has been found in the TNF-α promoter region; it has also been shown that lipopolysaccharide (LPS)-induced expression of TNF-α was mediated through the activation of Egr-1 by ERK1/2 in macrophage (Kramer et al., 1994; Shi et al., 2002). Our most recent study indicated that infection of primary mouse astrocytes with JHM also induced Egr-1 expression (Cai and Zhang, unpublished results). It remains to be seen whether Egr-1 is involved in regulation of TNF-α induction by MHV infection in these cells. In addition, it has been shown previously that there is a general correlation between MHV persistence and demyelination disease in the mouse CNS (Das Sarma et al., 2000), which is also correlated with the ability of MHV strains to induce Egr-1 expression as found in this study. However, a firm establishment of such a correlation requires further extensive experimentations in animals, i.e. using Egr-1 gene-knockout mice. Nevertheless, our current observation may offer some interesting clues for future investigation on the mechanism by which signal transduction pathways are differentially regulated by MHV strains.

Materials and methods

Viruses, cells, antibodies, and reagents

MHV strain JHM (Makino and Lai, 1989) was used throughout this study. In some experiments, MHV-A59 and MHV-2 strains were also used. These viruses were kindly provided by Dr. Michael Lai, and were propagated in the mouse astrocytoma DBT cell line (Hirano et al., 1974). DBT cells were also used for plaque assay and all other experiments involving cell culture throughout this study. DBT cells were cultured in 1×

minimum essential medium (MEM) containing 7.5% newborn calf serum (NCS) (Gibco), 10% trypton phosphate broth (TPB) and 1 mM of penicillin and streptomycin. Antibodies specific to mouse Egr-1 protein and β-actin were purchased from Santa Cruz Biochem. and Sigma, respectively. Antibodies specific to total ERK1/2 and phosphorylated ERK1/2 were ordered from Cell Signaling. MEK inhibitor UO126 was purchased from Cell Signaling, Inc. JNK inhibitor SP600125 and p38 inhibitor SB203580 were purchased from Calbiochem. ERK inhibitor CI-1040 was a gift of Pfizer, Inc. The siRNA specific to Egr-1 (Egr-1-siRNA) (Cat.# 040286-00) and to enhanced green fluorescence protein (EGFP-siRNA) (Cat.# 46-0926) were purchased from Dharmocon, Inc. and Invitrogen, respectively.

Reverse transcription and polymerase chain reaction (RT-PCR)

For detection of Egr-1 mRNAs, DBT cells were infected with MHV-JHM at a multiplicity of infection (m.o.i.) of 5, or mock-infected with serum-free medium. At various time points post-infection (p.i.), intracellular total RNAs were isolated and purified with the Trizol reagent (Invitrogen) according to the protocol from the manufacturer. RNAs were then treated with RNase-free DNase I (Promega) to remove the contaminated genomic DNAs. The concentrations of the RNA samples were determined by spectrophotometry (Hitatchi, Model 2100). Maloney murine leukemia virus (MMLV) reverse transcriptase (Promega) was used to reverse-transcribe the RNAs into cDNAs with a random hexomer oligonucleotide primer (Invitrogen) in a standard RT reaction as described previously (Zhang et al., 1991). cDNAs were then used as templates for PCR amplification with two pairs of primers specific for Egr-1 gene and β-actin gene (as an internal control), respectively. The sense primer for Egr-1 (5′Egr-1RT: 5′-ATG GCA GCG GCC AAG GCC-3′) corresponds to a sequence at nucleotide (nt) 1–18 of the open reading frame (ORF), and the anti-sense primer (3′Egr-1-RT: 5′-GGG TAC GGT TCT CCA GAC CCT-3′) is complementary to a sequence at nt 818–838 according to the published sequence (GenBank accession number: NM007913). The PCR product is 838 nt in length. The primer pair for β-actin is 5′mb-actin (5′-ACC AAC TGG GAC GAT ATG GAG AAG A-3′, corresponding to the sequence at nt 229–253) and 3′mb-actin (5′-TAC GAC CAG AGG CAT ACA GGG ACA-3′, complementary to a sequence at nt 418–442 of the β-actin gene) (GenBank accession number: NM007393). The PCR product for the β-actin gene is 214 nt in length. PCR was carried out in a reaction of 20 μl containing 1× PCR buffer (20 mM Tris–HCl, pH 8.3, 25 mM KCl, 1.5 mM MgCl$_2$, 0.1% Tween-20), 200 μM each of the four dNTPs, 20 pM of primers, 3 U of Taq DNA polymerase, and 2 μl of the RT products as templates for 30 cycles with each cycle consisting of denaturing at 95 °C for 20 s, annealing at 55 °C for 1 min, and extension at 72 °C for 1 min with a final extension of 10 min. PCR was performed in a thermocycler DNA Engine (Model PTC-200, MJ Research). PCR products were analyzed by agarose gel electrophoresis, and the gels were stained with ethidium bromide and photographed with a UVP gel document center.

UV inactivation of MHV

MHV-JHM strain was exposed to UV light for 20 min on ice in a UV-crosslinker (Fisher Scientific). Inactivation was confirmed by titration of samples in DBT cells before and after UV–light exposure, and by the absence of cytopathic effect after inoculation of DBT cell monolayers with UV-irradiated virus.

Western blot analysis

DBT cells were grown to monolayer in 60-mm Petri dishes and were infected with MHV strains JHM, A59, or MHV-2 or mock-infected with serum-free medium. At different time points p.i., cells were harvested and lysed in 50 µl of strong lysis buffer (25 mM HEPES, pH 7.5, 0.5% sodium deoxycholate, 1% Triton X-100, 0.2% SDS, 5 mM EDTA, 1 mM Na_3VO_4, 20 mM β-glycerophosphate, 50 mM NaF) containing protease inhibitor cocktail tablets (Roche). The lysates were sonicated 3 times for 20 s each on ice. The protein concentration was measured by using Bio-Rad protein assay kit (Bio-Rad, CA). Equal amounts of cell lysates were boiled for 5 min, chilled on ice, and pelleted by centrifugation before loading onto gels. Proteins were separated by SDS-polyacrylamide gel (10%) electrophoresis (PAGE). The proteins were then transferred to nitrocellulose membrane (MSI, Westborough, MA) for 7 h at 40 V in a transfer buffer (25 mM Tris, 200 mM glycine, 20% methanol, 0.02% SDS). After being blocked with 5% skim milk in Tris-buffered saline (TBS) for 1 h at room temperature (RT), the membrane was washed three times in TBS containing 0.5% Tween-20 and immunoblotted with a primary antibody (1 µg/ml) for 2 h at RT, followed by a secondary antibody coupled to horseradish peroxidase (1:1000 dilution) (Sigma) for 1 h at RT. The presence of the interested protein was detected by enhanced chemiluminescence (ECL) using peracid as a substrate (Amersham) followed by autoradiography.

Construction of plasmid DNA

For cloning of the Egr-1 gene, RNAs were isolated from DBT cells and cDNAs were synthesized by RT using the random hexamer primer as described above. The Egr-1 gene was amplified by PCR using the sense primer 5′Egr-1ORF (5′-TTT *GAA TTC* GGG ATG GCA GCG GCC AAG G-3′, corresponding to the first 16 nt of the Egr-1ORF, GenBank accession number NM007913), which contains an *Eco*RI site at the 5′-end (underlined), and the anti-sense primer 3′Egr-1ORF (5′-TTT *CTC GAG* GCA AAT TTC AAT TGT CCT GGG-3, complementary to the last 21 nt of the Egr-1 ORF), which contains an *Xho*I site (underlined). The PCR products were directly cloned into pCR2.1 TA cloning vector (Invitrogen), resulting in pTA-Egr-1. The sequence of the clone was confirmed by automatic DNA sequencing (IBI, Prizm-377) in the Departmental Core Facility. pTA-Egr-1 DNA was then digested with *Eco*RI and *Xho*I and directionally cloned into the *Eco*RI and *Xho*I sites of the plasmid

pcDNA3 (Invitrogen), generating pcDNA3/Egr-1. To generate pBS-CMV-Egr-1 plasmid, the pcDNA3/Egr-1 DNA was digested with *Eco*RI and *Xba*I and directionally cloned into the *Eco*RI and *Xba*I sites of the plasmid pBS-CMV.

DNA transfection and assays for luciferase and beta-galactosidase activities

For DNA transfection, the LipofectAmine reagent was used according to the manufacturer's instruction (Invitrogen). Briefly, DBT cells were seeded in a 24-well culture plates at a density of 4×10^5 cells per well. When the cells reached to approximately 60% confluency, ≈500 ng of plasmid DNAs and 3 µl of the LipofectAmine reagent were diluted separately in 100 µl of serum-free OPTI medium without antibiotics, mixed, and incubated at RT for 30 min before adding to each well of the 24-well plate. DBT cells were washed with PBS and 300 µl of OPTI medium was added to each well of the cell culture. The DNA-lipofectAmine mixture (200 µl) was added to each well and the cell culture plates were incubated at 37 °C for various time periods as indicated. For luciferase assay, cells were harvested along with culture medium and lysed by freezing and thawing. The cell lysate (100 µl) was assayed for luciferase activity using the luciferase assay system (Promega) in a microtiter plate luminometer (Dynex Technologies). For β-galactosidase assay, the medium was removed and the monolayers were washed twice with PBS after 24 h post-transfection. The cells were harvested into microfuge tubes by scraping the cells. The cells were recovered by centrifugation at 12,000×g for 10 s at RT. 125 µl lysis buffer (0.25 M Tris–HCl, pH 8.0) was added into the tubes. The cells were lysed by freezing at −70 °C and thawing at 37 °C three times. The cell extract was recovered by centrifuging at 12,000×g for 5 min at 4 °C. For each sample to be assayed, the following reagents were mixed together: 3 µl of 100× Mg solution (0.1 M MaCl2, 4.5 M β-mercaptoethanol), 66 µl of 1× ONPG (*o*-nitrophenyl-β-D-galactopyranoside), 30 µl of cell extract and 201 µl of 0.1 M sodium phosphate (pH 7.5). The reaction was incubated at 37 °C for 30 min. The reaction was then stopped by adding 500 µl of 1 M Na_2CO_3. The optical density of the reaction was read at a wavelength of 420 nm.

Detection of apoptotic cells

Apoptosis was determined by counting the apoptotic nuclei under a microscope following propidium iodide staining as described previously (Liu et al., 2003). Apoptosis was expressed as mean percentage of the cell population and standard deviation of three independent experiments.

Statistical analysis

The results are expressed as mean ± standard deviation (SD) and the mean values were compared using Student's *t* test. Values of $p < 0.05$, $p < 0.01$, and $p < 0.001$ were considered statistically significant.

Acknowledgments

References

Adami, C., Pooley, J., Glomb, J., Stecker, E., Fazal, F., Fleming, J.O., Baker, S.C., 1995. Evolution of mouse hepatitis virus (MHV) during chronic infection: quasispecies nature of the persisting MHV RNA. Virology 209, 337–346.

Banerjee, S., Narayanan, K., Mizutani, T., Makino, S., 2002. Murine coronavirus replication-induced p38 mitogen-activated protein kinase activation promotes interleukin-6 production and virus replication in cultured cells. J. Virol. 76, 5937–5948.

Baron, V., De Gregorio, G., Krones-Herzig, A., Virolle, T., Calogero, A., Urcis, R., Mercola, D., 2003a. Inhibition of Egr-1 expression reverses transformation of prostate cancer cells in vitro and in vivo. Oncogene 22, 4194–4204.

Baron, V., Duss, S., Rhim, J., Mercola, D., 2003b. Antisense to the early growth response-1 gene (Egr-1) inhibits prostate tumor development in TRAMP mice. Ann. N. Y. Acad. Sci. 1002, 197–216.

Bennett, B.L., Sasaki, D.T., Murray, B.W., O'Leary, E.C., Sakata, S.T., Xu, W., Leisten, J.C., Motiwala, A., Pierce, S., Satoh, Y., Bhagwat, S.S., Manning, A.M., Anderson, D.W., 2001. SP600125, an anthrapyrazolone inhibitor of Jun N-terminal kinase. Proc. Natl. Acad. Sci. U.S.A. 98, 13681–13686.

Biesiada, E., Razandi, M., Levin, E.R., 1996. Egr-1 activates basic fibroblast growth factor transcription. Mechanistic implications for astrocyte proliferation. J. Biol. Chem. 271, 18576–18581.

Bruick, R.K., 2000. Expression of the gene encoding the proapoptotic Nip3 protein is induced by hypoxia. Proc. Natl. Acad. Sci. U.S.A. 97, 9082–9087.

Cai, Y., Liu, Y., Yu, D., Zhang, X., 2003. Down-regulation of transcription of the proapoptotic gene BNip3 in cultured astrocytes by murine coronavirus infection. Virology 316, 104–115.

Calogero, A., Cuomo, L., D'Onofrio, M., de Grazia, U., Spinsanti, P., Mercola, D., Faggioni, A., Frati, L., Adamson, E.D., Ragona, G., 1996. Expression of Egr-1 correlates with the transformed phenotype and the type of viral latency in EBV genome positive lymphoid cell lines. Oncogene 13, 2105–2112.

Cao, X.M., Koski, R.A., Gashler, A., McKiernan, M., Morris, C.F., Gaffney, R., Hay, R.V., Sukhatme, V.P., 1990. Identification and characterization of the Egr-1 gene product, a DNA-binding zinc finger protein induced by differentiation and growth signals. Mol. Cell. Biol. 10, 1931–1939.

Cao, X.M., Guy, G.R., Sukhatme, V.P., Tan, Y.H., 1992. Regulation of the Egr-1 gene by tumor necrosis factor and interferons in primary human fibroblasts. J. Biol. Chem. 267, 1345–1349.

Changelian, P.S., Feng, P., King, T.C., Milbrandt, J., 1989. Structure of the NGFI-A gene and detection of upstream sequences responsible for its transcriptional induction by nerve growth factor. Proc. Natl. Acad. Sci. U.S.A. 86, 377–3781.

Chen, W., Baric, R.S., 1995. Function of a 5′-end genomic RNA mutation that evolves during persistent mouse hepatitis virus infection in vitro. J. Virol. 69, 7529–7540.

Chen, W., Baric, R.S., 1996. Molecular anatomy of mouse hepatitis virus persistence: coevolution of increased host cell resistance and virus virulence. J. Virol. 70, 3947–3960.

Chen, Y., Swanson, R.A., 2003. Astrocytes and brain injury. J. Cereb. Blood Flow Metab. 23, 137–149.

Christy, B., Nathans, D., 1989. Functional serum response elements upstream of the growth factor-inducible gene zif268. Mol. Cell. Biol. 9, 4889–4895.

Cuenda, A., Rouse, J., Doza, Y.N., Meier, R., Cohen, P., Gallagher, T.F., Young, P.R., Lee, J.C., 1995. SB 203580 is a specific inhibitor of a MAP kinase homologue which is stimulated by cellular stresses and interleukin-1. FEBS Lett. 364, 229–233.

Das Sarma, J., Fu, L., Tsai, J.C., Weiss, S.R., Lavi, E., 2000. Demyelination determinants map to the spike glycoprotein gene of coronavirus mouse hepatitis virus. J. Virol. 74, 9206–9213.

Delbridge, G.J., Khachigian, L.M., 1997. FGF-1-induced platelet-derived growth factor-A chain gene expression in endothelial cells involves transcriptional activation by early growth response factor-1. Circ. Res. 81, 282–288.

Eid, M.A., Kumar, M.V., Iczkowski, K.A., Bostwick, D.G., Tindall, D.J., 1998. Expression of early growth response genes in human prostate cancer. Cancer Res. 58, 2461–2468.

Favata, M.F., Horiuchi, K.Y., Manos, E.J., Daulerio, A.J., Stradley, D.A., Feeser, W.S., Van Dyk, D.E., Pitts, W.J., Earl, R.A., Hobbs, F., Copeland, R.A., Magolda, R.L., Scherle, P.A., Trzaskos, J.M., 1998. Identification of a novel inhibitor of mitogen-activated protein kinase kinase. J. Biol. Chem. 273, 18623–18632.

Fleming, J.O., Houtman, J.J., Alaca, H., Hinze, H.C., McKenzie, D., Aiken, J., Bleasdale, T., Baker, S., 1993. Persistence of viral RNA in the central nervous system of mice inoculated with MHV-4. Adv. Exp. Med. Biol. 342, 327–332.

Fu, Z.F., Weihe, E., Zheng, Y.M., Schafer, M.K., Sheng, H., Corisdeo, S., Rauscher, F.J., Koprowski, H., Dietzschold, B., 1993. Differential effects of rabies and borna disease viruses on immediate-early- and late-response gene expression in brain tissues. J. Virol. 67, 6674–6681.

Fujii, M., Niki, T., Mori, T., Matsuda, T., Matsui, M., Nomura, N., Seiki, M., 1991. HTLV-1 Tax induces expression of various immediate early serum responsive genes. Oncogene 6, 1023–1029.

Fujii, M., Tsuchiya, H., Chuhjo, T., Akizawa, T., Seiki, M., 1992. Interaction of HTLV-1 Tax1 with p67SRF causes the aberrant induction of cellular immediate early genes through CArG boxes. Genes Dev. 6, 2066–2076.

Grzybicki, D.M., Kwack, K.B., Perlman, S., Murphy, S.P., 1997. Nitric oxide synthase type II expression by different cell types in MHV-JHM encephalitis suggests distinct roles for nitric oxide in acute versus persistent virus infection. J. Neuroimmunol. 73, 15–27.

Harrington, M.A., Edenberg, H.J., Saxman, S., Pedigo, L.M., Daub, R., Broxmeyer, H.E., 1991. Cloning and characterization of the murine promoter for the colony-stimulating factor-1-encoding gene. Gene 102, 165–170.

Herndon, R.M., Griffin, D.E., McCormick, U., Weiner, L.P., 1975. Mouse hepatitis virus-induced recurrent demyelination. Arch. Neurol. 32, 32–35.

Herndon, R.M., Price, D.L., Weiner, L.P., 1977. Regeneration of oligodendroglia during recovery from demyelinating disease. Science 195, 693–694.

Hill, C.S., Treisman, R., 1995. Transcriptional regulation by extracellular signals: mechanisms and specificity. Cell 80, 199–211.

Hirano, N., Fujiwara, K., Hino, S., Matumoto, M., 1974. Replication and plaque formation of mouse hepatitis virus (MHV-2) in mouse cell line DBT culture. Arch. Gesamte Virusforsch. 44, 298–302.

Honkaniemi, J., Sagar, S.M., Pyykonen, I., Hicks, K.J., Sharp, F.R., 1995. Focal brain injury induces multiple immediate early genes encoding zinc finger transcription factors. Brain Res. Mol. Brain Res. 28, 157–163.

Huang, D., Han, Y., Rani, M.R., Glabinski, A., Trebst, C., Sorensen, T., Tani, M., Wang, J., Chien, P., O'Bryan, S., Bielecki, B., Zhou, Z.L., Majumder, S., Ransohoff, R.M., 2000. Chemokines and chemokine receptors in inflammation of the nervous system: manifold roles and exquisite regulation. Immunol. Rev. 177, 52–67.

Hu, R.M., Levin, E.R., 1994. Astrocyte growth is regulated by neuropeptides through Tis 8 and basic fibroblast growth factor. J. Clin. Invest. 93, 1820–1827.

James, A.B., Conway, A.M., Thiel, G., Morris, B.J., 2004. Egr-1 modulation of synapsin I expression: permissive effect of forskolin via cAMP. Cell. Signal. 16, 1355–1362.

Joseph, J., Grun, J.L., Lublin, F.D., Knobler, R.L., 1993. Interleukin-6 induction in vitro in mouse brain endothelial cells and astrocytes by exposure to mouse hepatitis virus (MHV-4, JHM). J. Neuroimmunol. 42, 47–52.

Kalicharran, K., Mohandas, D., Wilson, G., Dales, S., 1996. Regulation of the initiation of coronavirus JHM infection in primary oligodendrocytes and L-2 fibroblasts. Virology 225, 33–43.

Khachigian, L.M., Lindner, V., Williams, A.J., Collins, T., 1996. Egr-1-induced endothelial gene expression: a common theme in vascular injury. Science 271, 1427–1431.

Kobayashi, D., Yamada, M., Kamagata, C., Kaneko, R., Tsuji, N., Nakamura, M., Yagihashi, A., Watanabe, N., 2002. Overexpression of early growth response-1 as a metastasis-regulatory factor in gastric cancer. Anticancer Res. 22, 3963–3970.

Kramer, B., Meichle, A., Hensel, G., Charnay, P., Kronke, M., 1994. Characterization of an Krox-24/Egr-1-responsive element in the human tumor necrosis factor promoter. Biochim. Biophys. Acta 1219, 413–421.

Kyuwa, S., Cohen, M., Nelson, G., Tahara, S.M., Stohlman, S.A., 1994. Modulation of cellular macromolecular synthesis by coronavirus: implication for pathogenesis. J. Virol. 68, 6815–6819.

Lampert, P.W., Sims, J.K., Kniazeff, A.J., 1973. Mechanism of demyelination in JHM virus encephalomyelitis. Acta. Neuropathol. 24, 76–85.

Lemaire, P., Vesque, C., Schmitt, J., Stunnenberg, H., Frank, R., Charnay, P., 1990. The serum-inducible mouse gene Krox-24 encodes a sequence-specific transcriptional activator. Mol. Cell. Biol. 10, 3456–3467.

Li, Y., Fu, L., Gonzales, D.M., Lavi, E., 2004. Coronavirus neurovirulence correlates with the ability of the virus to induce proinflammatory cytokine signals from astrocytes and microglia. J. Virol. 78, 3398–3406.

Lim, C.P., Jain, N., Cao, X., 1998. Stress-induced immediate-early gene, egr-1, involves activation of p38/JNK1. Oncogene 16, 2915–2926.

Liu, Y., Zhang, X., 2005. Expression of cellular oncogene Bcl-xL prevents coronavirus-induced cell death and converts acute infection to persistent infection in progenitor rat oligodendrocytes. J. Virol. 79, 47–56.

Liu, Y., Cai, Y., Zhang, X., 2003. Induction of caspase-dependent apoptosis in cultured rat oligodendrocytes by murine coronavirus is mediated during cell entry and does not require virus replication. J. Virol. 77, 11952–11963.

Maeda, A., Hayashi, M., Ishida, K., Mizutani, T., Watanabe, T., Namioka, S., 1995. Characterization of DBT cell clones derived from cells persistently infected with the JHM strain of mouse hepatitis virus. J. Vet. Med. Sci. 57, 813–817.

Makino, S., Lai, M.M.C., 1989. Evolution of the 5′-end of genomic RNA of murine coronaviruses during passages in vitro. Virology 169, 227–232.

Maltzman, J.S., Carmen, J.A., Monroe, J.G., 1996. Transcriptional regulation of the Icam-1 gene in antigen receptor- and phorbol ester-stimulated B lymphocytes: role for transcription factor EGR1. J. Exp. Med. 183, 1747–1759.

Matsuyama, S., Taguchi, F., 2002. Receptor-induced conformational changes of murine coronavirus spike protein. J. Virol. 76, 11819–11826.

McGilvray, I.D., Lu, Z., Wei, A.C., Dackiw, A.P., Marshall, J.C., Kapus, A., Levy, G., Rotstein, O.D., 1998. Murine hepatitis virus strain 3 induces the macrophage prothrombinase fgl-2 through p38 mitogen-activated protein kinase activation. J. Biol. Chem. 273, 32222–32229.

Milbrandt, J., 1987. A nerve growth factor-induced gene encodes a possible transcriptional regulatory factor. Science 238, 797–799.

Nash, T.C., Buchmeier, M.J., 1997. Entry of mouse hepatitis virus into cells by endosomal and nonendosomal pathways. Virology 233, 1–8.

Nguyen, H.Q., Hoffman-Liebermann, B., Liebermann, D.A., 1993. The zinc finger transcription factor Egr-1 is essential for and restricts differentiation along the macrophage lineage. Cell 72, 197–209.

Perlman, S., Ries, D., 1987. The astrocyte is a target cell in mice persistently infected with mouse hepatitis virus strain JHM. Microb. Pathog. 3, 309–314.

Porntadavity, S., Xu, Y., Kiningham, K., Rangnekar, V.M., Prachayasitikul, V., St Clair, D.K., 2001. TPA-activated transcription of the human MnSOD gene: role of transcription factors Sp-1 and Egr-1. DNA Cell Biol. 20, 473–481.

Rowe, C.L., Baker, S.C., Nathan, M.J., Sgro, J.Y., Palmenberg, A.C., Fleming, J.O., 1998. Quasispecies development by high frequency RNA recombination during MHV persistence. Adv. Exp. Med. Biol. 440, 759–765.

Sakamoto, K.M., Nimer, S.D., Rosenblatt, J.D., Gasson, J.C., 1992. HTLV-I and HTLV-II tax transactivate the human EGR-1 promoter through different cis-acting sequences. Oncogene 7, 2125–2130.

Santiago, F.S., Lowe, H.C., Day, F.L., Chesterman, C.N., Khachigian, L.M., 1999. Early growth response factor-1 induction by injury is triggered by release and paracrine activation by fibroblast growth factor-2. Am. J. Pathol. 154, 937–944.

Sawicki, S.G., Lu, J.H., Holmes, K.V., 1995. Persistent infection of cultured cells with mouse hepatitis virus (MHV) results from the epigenetic expression of the MHV receptor. J. Virol. 69, 5535–5543.

Sebesteny, A., Hill, A.C., 1974. Hepatitis and brain lesions due to mouse hepatitis virus accompanied by wasting in nude mice. Lab. Anim. 8, 317–326.

Sebolt-Leopold, J.S., Dudley, D.T., Herrera, R., Van Becelaere, K., Wiland, A., Gowan, R.C., Tecle, H., Barrett, S.D., Bridges, A., Przybranowski, S., Leopold, W.R., Saltiel, A.R., 1999. Blockade of the MAP kinase pathway suppresses growth of colon tumors in vivo. Nat. Med. 5, 810–816.

Shi, L., Kishore, R., McMullen, M.R., Nagy, L.E., 2002. Lipopolysaccharide stimulation of ERK1/2 increases TNF-alpha production via Egr-1. Am. J. Physiol.: Cell Physiol. 282, 1205–1211.

Skerka, C., Decker, E.L., Zipfel, P.F., 1995. A regulatory element in the human interleukin 2 gene promoter is a binding site for the zinc finger proteins Sp1 and EGR-1. J. Biol. Chem. 270, 22500–22506.

Sukhatme, V.P., Cao, X.M., Chang, L.C., Tsai-Morris, C.H., Stamenkovich, D., Ferreira, P.C., Cohen, D.R., Edwards, S.A., Shows, T.B., Curran, T., Le Beau, M.M., Adamson, E.D., 1988. A zinc finger-encoding gene coregulated with c-fos during growth and differentiation, and after cellular depolarization. Cell 53, 37–43.

Sun, Y., Huang, P.L., Li, J.J., Huang, Y.Q., Zhang, L., Huang, P.L., Lee-Huang, S., 2001. Anti-HIV agent MAP30 modulates the expression profile of viral and cellular genes for proliferation and apoptosis in AIDS-related lymphoma cells infected with Kaposi's sarcoma-associated virus. Biochem. Biophys. Res. Commun. 287, 983–994.

Suzuki, T., Fujisawa, J.I., Toita, M., Yoshida, M., 1993. The trans-activator tax of human T-cell leukemia virus type 1 (HTLV-1) interacts with cAMP-responsive element (CRE) binding and CRE modulator proteins that bind to the 21-base-pair enhancer of HTLV-1. Proc. Natl. Acad. Sci. U.S.A. 90, 610–614.

Van Wagoner, N.J., Benveniste, E.N., 1999. Interleukin-6 expression and regulation in astrocytes. J. Neuroimmunol. 100, 124–139.

Varnum, B.C., Lim, R.W., Kujubu, D.A., Luner, S.J., Kaufman, S.E., Greenberger, J.S., Gasson, J.C., Herschman, H.R., 1989. Granulocyte-macrophage colony-stimulating factor and tetradecanoyl phorbol acetate induce a distinct, restricted subset of primary-response TIS genes in both proliferating and terminally differentiated myeloid cells. Mol. Cell. Biol. 9, 3580–3583.

Virolle, T., Krones-Herzig, A., Baron, V., De Gregorio, G., Adamson, E.D., Mercola, D., 2003. Egr1 promotes growth and survival of prostate cancer cells. Identification of novel Egr1 target genes. J. Biol. Chem. 278, 11802–11810.

Wagner, A., Doerks, A., Aboud, M., Alonso, A., Tokino, T., Flugel, R.M., Lochelt, M., 2000. Induction of cellular genes is mediated by the Bel1 transactivator in foamy virus-infected human cells. J. Virol. 74, 4441–4447.

Waters, C.M., Hancock, D.C., Evan, G.I., 1990. Identification and characterisation of the egr-1 gene product as an inducible, short-lived, nuclear phosphoprotein. Oncogene 5, 669–674.

Williams, R.K., Jiang, G.S., Holmes, K.V., 1991. Receptor for mouse hepatitis virus is a member of the carcinoembryonic antigen family of glycoproteins. Proc. Natl. Acad. Sci. U.S.A. 88, 5533–5536.

Woyciechowska, J.L., Trapp, B.D., Patrick, D.H., Shekarchi, I.C., Leinikki, P.O., Sever, J.L., Holmes, K.V., 1984. Acute and subacute demyelination induced by mouse hepatitis virus strain A59 in C3H mice. J. Exp. Pathol. 1, 295–306.

Wright, J.J., Gunter, K.C., Mitsuya, H., Irving, S.G., Kelly, K., Siebenlist, U., 1990. Expression of a zinc finger gene in HTLV-I- and HTLV-II-transformed cells. Science 248, 588–591.

Yu, D.D., Zhang, X.M., in press. Differential induction of proinflammatory cytokines in primary mouse astrocytes and microglia by coronavirus infection. In: Perlman, S., Holmes, K.V. (eds.), The Nidoviruses: The Control of SARS and Other Nidovirus diseases. Springer.

Zhang, X.M., Kousoulas, K.G., Storz, J., 1991. Comparison of the nucleotide and deduced amino acid sequences of the S genes specified by virulent and avirulent strains of bovine coronaviruses. Virology 183, 397–404.

Zhou, J., Stohlman, S.A., Marten, N.W., Hinton, D.R., 2001. Regulation of matrix metalloproteinase (MMP) and tissue inhibitor of matrix metalloproteinase (TIMP) genes during JHMV infection of the central nervous system. Adv. Exp. Med. Biol. 494, 329–334.